SHORT PAPERS

TURNING OF SLENDER WORKPIECES: MODELING AND EXPERIMENTS

R. Katz, C. W. Lee,† A. G. Ulsoy and R. A. Scott

Department of Mechanical Engineering and Applied Mechanics, The University of Michigan, Ann Arbor, Michigan 48109, U.S.A.

This paper introduces a dynamic cutting force model for turning of slender workpieces, as well as experimental results related to the frequency response of the workpiece in turning. The model is based on a flexible workpiece and rigid machine tool, and a workpiece displacement dependent cutting force. The model is described and studied theoretically as well as experimentally. The experimental studies utilise both cutting force and workpiece vibration measurements in two orthogonal directions. This data is obtained for both cutting and non-cutting conditions, and analysed in the frequency domain. The model was found to be in partial agreement with the experimental results. The experimental procedure described here represents a new method for determining the cutting process damping ratio, based on differences in the measured workpiece natural frequencies with and without cutting.

1. INTRODUCTION

In this paper we introduce a new dynamic cutting force model for the turning process of a slender workpiece, as well as some experimental results related to the frequency response of this system.

Traditional models of the cutting process consider a rigid workpiece and vibration of the machine tool structure [11, 12]. These vibrations result in the actual depth of cut (d) deviating from the nominal value (d_0). Since the cutting force component in the tool axis is proportional to the actual depth of cut, it has a component which depends on the machine tool dynamics. There is also the so-called "regenerative effect" where workpiece surface undulations caused by structural vibrations during a previous pass cause deviations from the nominal depth of cut. This effect is characterised by the overlap factor ($0 \leqslant \mu \leqslant 1$) and the time delay ($T$). These are summarised in a schematic block diagram in Fig. 1 [8]. In this figure (P) is the cutting force and (U) is the relative displacement (the response).

There are several models proposed to describe the cutting process dynamics. For example, Merrit [8], and Gurney and Tobias [3], have modeled the dynamic cutting process by a proportional relationship $\delta P = kU$, where δP is the variation of the cutting force from its steady state value. Tobias and Fishwick [12] have suggested relations which include $\dot{U}$, and thus introduce process damping, $\delta P = -k_1 U - k_2 \dot{U}$, while Hanna and Tobias [4] have employed the non-linear equation $\delta P = k_1 U + k_2 U^2 + k_3 U^3$.

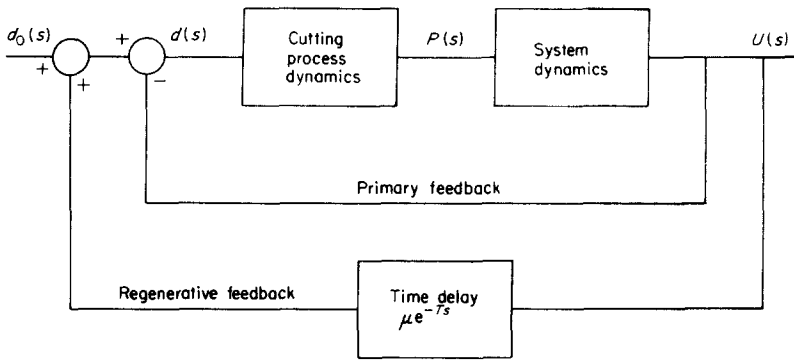† Visiting Professor, Korea Advanced Institute of Science and Technology.

Figure 1. Block diagram of a dynamic cutting process model.

The system dynamics block in Fig. 1 usually represents the machine tool dynamics and is often characterised by $(U(s)/P(s)) = (G_m(s)/K_m)$ where K_m is the static structural stiffness and $G_m(s)$ represents the dynamic compliance. Note that the workpiece dynamics is not considered in this model, and a lumped parameter model of the structure is used.

In turning of long slender workpieces it is appropriate to assume a rigid machine tool structure and a flexible model of the workpiece. We have studied such systems using a rotating shaft model of the workpiece subject to axially traveling cutting loads [6, 7]. Those studies have shown that an Euler–Bernoulli beam model is adequate for conventional machining, and that the dynamic effects due to rotational speed and feedrate are only significant for ultra high speed and ballistic machining [2]. We also note that there is some support [10] for the notion that while process damping is important in conventional machining, it becomes less significant in high speed machining.

In this paper, based on the results of our previous studies [6, 7], we introduce a model suitable for describing the dynamics of conventional turning of long slender workpieces. The model is used to predict expected changes in the workpiece natural frequencies during cutting. Experiments were performed to validate the model, and the results partially confirm the model predictions. The experiments and model also provide a convenient method for determining the process damping.

2. THEORY

2.1. DYNAMIC CUTTING FORCE MODEL

The dynamic cutting force model used here is an extension of the model in Katz *et al.* [6] in that it includes process damping.

In the derivation of the model the following assumptions have been made (see Fig. 2).

(1) The frame of the machine tool and the tool are rigid with respect to the workpiece, which is assumed to be flexible in the lateral direction.

(2) The relative displacements between the workpiece and the tool frame are considered.

(3) The actual depth of cut is dependent only on the horizontal displacement (U_1).

(4) Only planar force components (P_1 and P_2) in a plane perpendicular to the axis of the workpiece are included.

(5) The cutting forces are modeled using the elementary cutting force equations [1]
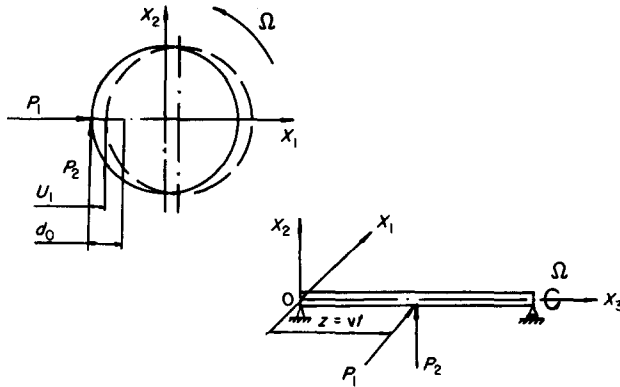
$$P = Kd^\alpha f^\beta. \tag{1}$$

Figure 2. The dynamic cutting force model.

The actual depth of cut is $d = d_0 - U_1$ (see Fig. 2). Therefore, using equation (1) one can write the force components as,

$$P_1 = K_A f^{\beta_1}(d_0 - U_1)^{\alpha_1}$$
$$P_2 = K_B f^{\beta_2}(d_0 - U_1)^{\alpha_2}. \tag{2}$$

Expanding in a binomial series and keeping only first order terms, one obtains:

$$P_1 \simeq \bar{P}_1 - K_1 U_1 = \bar{P}_1 - \delta P_1$$
$$P_2 \simeq \bar{P}_2 - K_2 U_1 = \bar{P}_2 - \delta P_2 \tag{3}$$

where,

$$\bar{P}_1 = K_A f^{\beta_1} d_0^{\alpha_1}$$
$$\bar{P}_2 = K_B f^{\beta_2} d_0^{\alpha_2} \tag{4}$$

and,

$$K_1 = (\alpha_1 K_A / d_0) f^{\beta_1} d_0^{\alpha_1} = (\alpha_1 / d_0) \bar{P}_1$$
$$K_2 = (\alpha_2 K_B / d_0) f^{\beta_2} d_0^{\alpha_2} = (\alpha_2 / d_0) \bar{P}_2. \tag{5}$$

The cutting force coefficients (K_A, K_B) can be determined experimentally. The values of f and d_0 are nominal values to be set on the machine. It is important to note that in the model suggested here both cutting force components, δP_1 and δP_2, are dependent on U_1 only.

As mentioned previously the above model, which does not include damping terms, may be adequate to describe the cutting forces at very high speeds of machining. However, in order to describe cutting in conventional stable turning operations, velocity dependent terms which represent process damping should be included in the model. Therefore the extended cutting force model to be used here is,

$$P_1 = \bar{P}_1 - K_1 U_1 - C_1 \dot{U}_1$$
$$P_2 = \bar{P}_2 - K_2 U_1 - C_2 \dot{U}_1. \tag{6}$$

The velocity dependent terms represent the overall damping effects due to cutting and again they are assumed to be dependent on the $\dot{U}_1$ component only.

2.2. THE DYNAMIC MODEL OF THE WORKPIECE

Based on the studies in Katz *et al.* [7] the workpiece is treated as a rotating, simply supported shaft, and Euler–Bernoulli beam theory is considered adequate. The equations of motion are (see Fig. 2):

$$EI \frac{\partial^4 U_1}{\partial z^4} + \rho A \frac{\partial^2 U_1}{\partial t^2} = P_1(z, t)$$

$$EI \frac{\partial^4 U_2}{\partial z^4} + \rho A \frac{\partial^2 U_2}{\partial t^2} = P_2(z, t). \tag{7}$$

The applied cutting forces are assumed to move at a constant axial (feed) velocity (v). Here the analysis is restricted to very low axial speeds such as those in conventional turning. Then equations (7), using equations (6), may be written in the form,

$$EI \frac{\partial^4 U_1}{\partial z^4} + \rho A \frac{\partial^2 U_1}{\partial t^2} + K_1 U_1(z_i, t) + C_1 \dot{U}_1(z_i, t) = \bar{P}_1(z_i)$$

$$EI \frac{\partial^4 U_2}{\partial z^4} + \rho A \frac{\partial^2 U_2}{\partial t^2} + K_2 U_1(z_i, t) + C_2 \dot{U}_1(z_i, t) = \bar{P}_2(z_i) \tag{8}$$

where z_i is the location of the load.

2.3. THE APPROXIMATE SOLUTION METHOD

Galerkin's method is used to obtain an approximate solution to equations (8). For a simply-supported workpiece, and a one term approximation with a comparison function $\sin(\pi z/l)$ we take $U_1 = g_1(t) \sin(\pi z/l)$ and $U_2 = g_2(t) \sin(\pi z/l)$. Galerkin's method yields the constant coefficient differential equations,

$$\begin{Bmatrix} \ddot{g}_1 \\ \ddot{g}_2 \end{Bmatrix} + \begin{bmatrix} C_1^* & 0 \\ C_2^* & 0 \end{bmatrix} \begin{Bmatrix} \dot{g}_1 \\ \dot{g}_2 \end{Bmatrix} + \begin{bmatrix} (\omega_1^2 + K_1^*) & 0 \\ K_2^* & \omega_1^2 \end{bmatrix} \begin{Bmatrix} g_1 \\ g_2 \end{Bmatrix} = \begin{Bmatrix} P_1^* \\ P_2^* \end{Bmatrix} \tag{9}$$

or,

$$[I]\mathbf{g} + [C]\dot{\mathbf{g}} + [K]\mathbf{g} = \mathbf{P}^* \tag{10}$$

where:

$$\omega_1^2 = (\pi/l)^4 (EI/\rho A)$$

$$C_k^* = (2C_k/\rho Al) \sin^2(\pi/l)z_i; \qquad (k = 1, 2)$$

$$K_k^* = (2K_k/\rho Al) \sin^2(\pi/l)z_i; \qquad (k = 1, 2) \tag{11}$$

$$P_k^* = (2P_k/\rho Al) \sin(\pi/l)z_i; \qquad (k = 1, 2).$$

Let us consider the homogeneous part of equation (9). The damped natural frequencies are the solution of the eigenvalue problem, and the characteristic determinant has the form,

$$\det \begin{bmatrix} \lambda^2 + C_1^* \lambda + (\omega_1^2 + K_1^*) & 0 \\ C_2^* \lambda + K_2^* & \lambda^2 + \omega_1^2 \end{bmatrix} = 0. \tag{12}$$

The solution of equation (12) leads to the values of λ,

$$\lambda_{1,2} = \pm i\omega_1 \tag{13}$$

and,

$$\lambda_{3,4} = -\zeta \omega_n \pm i\omega_n \sqrt{1 - \zeta^2} \tag{14}$$

where,

$$\zeta = C_1^*/(2\sqrt{\omega_1^2 + K_1^*})$$
$$\omega_n = \sqrt{\omega_1^2 + K_1^*}. \tag{15}$$

It is important to note, that C_2^* and K_2^*, which are the cutting process coefficients in the direction perpendicular to the tool, have no effect on the natural frequencies of the system. This is a result of the assumption in equations (2) and (6) that P_1 and P_2 depend only on U_1 and $\dot{U}_1$, but not on U_2 and $\dot{U}_2$. Consider the following special cases.

Case 1. Assume that there is no damping in the process, $C_1^* = C_2^* = 0$, (such as in high speed machining). In this case the eigenvalues $\lambda_{1,2}$ are the same as in equation (13) and,

$$\lambda_{3,4} = \pm i\sqrt{\omega_1^2 + K_1^*}. \tag{16}$$

The physical interpretation of equations (13) and (16) is that in the plane of the tool there exists a stiffening effect due to the cutting process, while in the perpendicular direction one may expect to obtain the natural frequency of an unconstrained Euler-Bernoulli beam, which is independent of the cutting process.

The fundamental frequency of vibration in the OX_1 direction, when the tool is located at the midspan of the workpiece ($z_i = l/2$), is obtained by using equation (16),

$$\omega_{21} = \sqrt{(\pi/l)^4(EI/\rho A) + (2K_1/\rho Al)} \tag{17}$$

while in the OX_2 direction the natural frequency is obtained according to equation (13)

$$\omega_{11} = (\pi/l)^2\sqrt{EI/\rho A}. \tag{18}$$

This "stiffening effect" of the natural frequency in the OX_1 direction is shown in the upper two curves of Fig. 3. The results in the upper two curves in Fig. 3 should be interpreted in the following manner: at each discrete location z_i of the cutting tool along the workpiece, two natural frequencies are expected to be observed while cutting. These are the unconstrained beam natural frequency ω_{11} as given in equation (18), and the "stiffened" frequency ω_{21} as given in equation (17).

Case 2. Next, assume that the process damping is introduced in the cutting model. According to equations (14) and (15) at $z_i = l/2$, the damped natural frequency of the
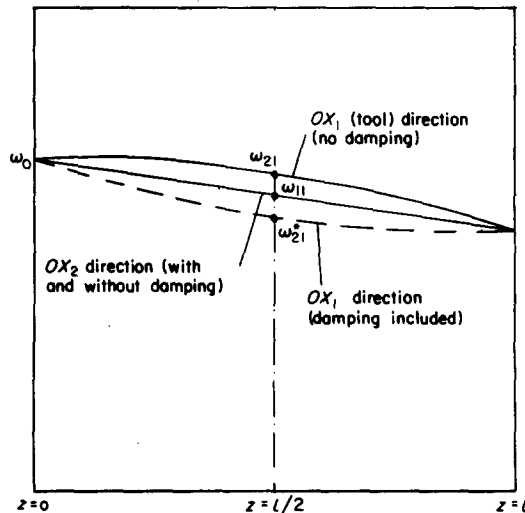

Figure 3. The predicted natural frequencies at some locations z_i of the tool (with and without damping).

system in the OX_1 direction is,

$$\omega_{21}^* = \omega_{21}\sqrt{1-\zeta^2}$$ (19)

where ω_{21} is given by equation (17) and the damping ratio is,

$$\zeta = \sqrt{C_1/(\omega_{21}\rho Al)}.$$ (20)

The frequency in the OX_2 direction is independent of the damping and remains ω_{11}. Note that process damping effects only ω_{21} and not ω_{11} due to the assumption in equation (6). The frequency ω_{21}^* is also shown in Fig. 3.

3. EXPERIMENTAL SETUP AND PROCEDURE

3.1. THE EXPERIMENTAL SETUP

The experimental setup is illustrated schematically in Fig. 4. Some properties of the workpiece and the cutting tool are summarised in Table 1. The lathe was a 15 HP conventional lathe. The cutting tool was mounted in a 3-axis dynamometer (with all fundamental natural frequencies above 1000 Hz). The lateral vibrations of the workpiece
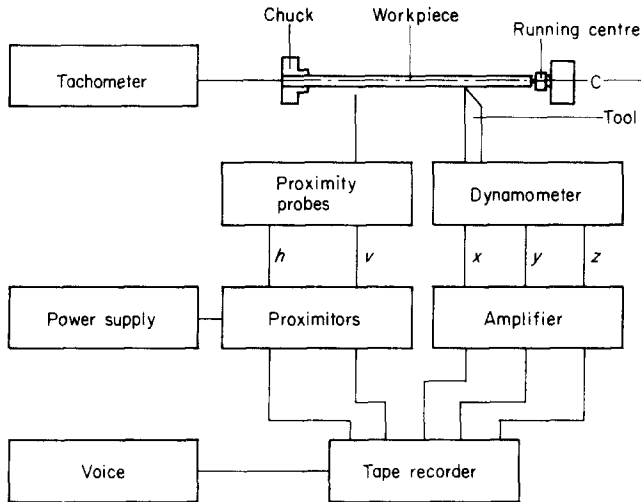
Figure 4. The experimental setup.

TABLE 1

Some properties of the workpiece and the tool

The cutting tool	
Material	H.S.S.
Rake angle	$<14°$
Relief angle	$7°$
The slender workpiece	
Material	Cold drawn steel, AISI-1020
Mass density	$\rho = 7700 \text{ kg/m}^3$
Nominal length	$l_1 = 0.865$ m (experiments 1)
	$l_2 = 0.675$ m (experiments 2)
Cross section area	$A = 1.14 \times 10^{-3} \text{ m}^2$

relative to the lathe were measured by two proximity probes which have a linear range of 1·5 mm, and which were located in the vertical and horizontal directions. The cutting force signals in the radial, vertical and axial directions and the signals from the proximity probes were recorded on five parallel F.M. channels of an instrumentation tape-recorder.

3.2. THE EXPERIMENTAL PROCEDURE

Two series of experiments were performed.

(1) Two workpieces of length $l = 0·865$ m.

(2) A workpiece of length $l = 0·675$ m.

In both series of experiments a second cut was usually performed to check if the regenerative chatter arose, and none was observed. Each experiment was divided into three steps:

(1) *Precutting.* Measurements of the natural frequency of the workpiece (without cutting), in the vertical and horizontal directions, using an impact hammer to excite the vibration. In addition, the signature of a rotating workpiece without cutting was measured in order to observe any possible noise signals due to the operation of the lathe.

(2) *Cutting.* Measurements of the cutting force signals, as well as the signals from the proximity probes. Impact hammer excitation was also used during a portion of the cutting test in order to fully excite the vibrations.

(3) *Post cutting.* Repetition of the same measurements as in the precutting part, after the cutting was completed.

In addition, a set of preliminary experiments were performed in order to experimentally evaluate the values of the cutting coefficients and exponents.

The stored data from both the proximity probes and from the dynamometer was analysed using an HP-3582-A spectrum analyser.

The signal analysis of the cutting experiments included the following steps.

(1) Determining individual power spectral densities (PSD) for each of the five channels in the range 0–250 Hz (frequency resolution of 1 Hz) using a Hanning window, and using 16–64 averages according to the available length of the data.

(2) Using "zoom" in the interesting range of frequencies to obtain higher resolution (up to 400 mHz).

(3) Finding the transfer function between the signal from the proximity probe and the corresponding dynamometer channel. In the interesting range of frequencies (115–135 Hz) the coherence function between the two signals was in the range 0·85–0·95, which indicates meaningful measurements.

4. RESULTS AND DISCUSSION

4.1. VALUES OF THE CUTTING FORCE COEFFICIENTS AND EXPONENTS

The results of the preliminary experiments are summarised in Table 2. The cutting coefficients and exponents were measured and evaluated using the method suggested in

TABLE 2

Results of the preliminary experiments

Variable	Direction OX_1 (radial)	OX_2 (tangential)
α_i	$\alpha_1 = 1·15 + 0·01$	$\alpha_2 = 0·75 \pm 0·10$
β_i	$\beta_1 = 0·53 \pm 0·05$	$\beta_2 = 0·36 \pm 0·05$
K_i N/m	$K_1 = 1·308 \times 10^5$	$K_2 = 9·411 \times 10^5$

Datsko [1]. The values of the coefficients K_1, K_2 were calculated using equations (5) and represent average values of these measurements. The nominal values of α and β were obtained using linear curve fitting based on repeated measurements of the cutting force vs. the feed and the depth of cut respectively.

4.2. MEASURED NATURAL FREQUENCIES

The data for each experiment is summarised in Table 3. Figure 5 represents a combined PSD plot of the results from the post-cutting and the cutting stages in experiment 3. The data was measured using the horizontal proximity probe and represents vibrations in the OX_1 direction. The number of averages used was 32, and the cutting signal was obtained on a logarithmic amplitude scale while the post-cutting signal is on a linear one.

The results verify the existence of a natural frequency which is related directly to the cutting process (i.e., not the free shaft frequency). This frequency is lower than the natural frequency of the shaft. The results of the measured natural frequency in each experiment are summarised in Table 4. All repeated measurements of the recorded data are within $\pm0\cdot5$ Hz about the nominal.

To summarise the results, the following findings may be stated.

(1) The cutting process, causes a decrease in the natural frequency of the workpiece, when compared with the natural frequency of the same workpiece without cutting. This

TABLE 3

Experimental data

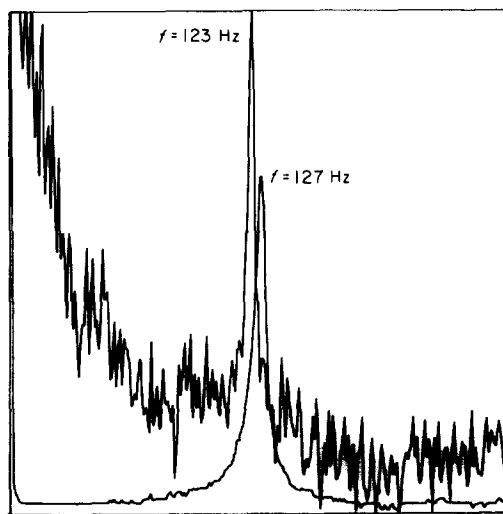| Experiment No.	l (m)	A (m²)	n (rpm)	d_0 (m)	f (m/rev)
1. First cut	0·865	$1\cdot14 \times 10^{-3}$	168	$1\cdot2 \times 10^{-3}$	$0\cdot5 \times 10^{-3}$
2. Second cut	0·865	$1\cdot0 \times 10^{-3}$	313	$1\cdot0 \times 10^{-3}$	$1\cdot0 \times 10^{-3}$
3. First cut	0·865	$1\cdot14 \times 10^{-3}$	171	$1\cdot1 \times 10^{-3}$	$0\cdot5 \times 10^{-3}$
4. Second cut	0·865	$1\cdot01 \times 10^{-3}$	170	$1\cdot15 \times 10^{-3}$	$0\cdot5 \times 10^{-3}$
5. First cut	0·675	$1\cdot14 \times 10^{-3}$	165	$1\cdot1 \times 10^{-3}$	$0\cdot5 \times 10^{-3}$
6. Second cut	0·675	$1\cdot01 \times 10^{-3}$	165	$1\cdot1 \times 10^{-3}$	$0\cdot5 \times 10^{-3}$

Figure 5. Superposition of cutting and post cutting frequency measurements from experiment 3.

TABLE 4

Nominal measurements of natural frequency

Experiment No.	Precutting frequency (H_z)		Cutting frequency (H_z)		Postcutting frequency (H_z)	
	Vertical	Horizontal	Vertical	Horizontal	Vertical	Horizontal
1. First cut	129	129	123	123	126	126
2. Second cut	126	126	122·5	122·5	Unrecorded	Unrecorded
3. First cut	130	130	123	123	127	127
4. Second cut	127	127	121·5	121·5	124·5	124·5
5. First cut	193	194	183	183	191	192
6. Second cut	191	192	185	185	187·5	Unrecorded

fact is shown in Fig. 5, and was a clear and consistent observation from all the experiments. It can be explained by the proposed model with damping.

(2) In all the cutting experiments, when four or more averages were used to obtain the PSD, one could not consistently observe two distinct natural frequencies (ω_{21}^* and ω_{11}) during the cutting process, as predicted by the model. However, two distinct frequencies consistent with the model predictions could be observed in some instantaneous spectra for all experiments. Further research is required, and a key issue is whether the vibrations during cutting can be assumed to be a stationary process.

4.3. DISCUSSION

In a model where damping is not included, one would expect to obtain a frequency ω_{21} which is higher than ω_{11}, according to equations (17) and (18), due to the fact that the cutting force introduces a stiffening effect. However, the results shown in Table 3 indicate that the measured frequency during cutting is lower than the frequency of the workpiece. Damping may explain this fact as ω_{21}^* is lower than ω_{11}. An issue is, what value of the damping ratio (ζ) would be required to match the experimental observations. From equation (19) one obtains,

$$\zeta = \sqrt{1 - \left(\frac{\omega_{21}^*}{\omega_{21}}\right)^2}. \tag{21}$$

Based on the results from Table 4 the values of ζ for each experiment are summarised in Table 5. The range of the calculated nominal values of ζ is 0·22–0·33. These are reasonable values when a stable (chatter free) cutting operation is taking place, and so damping can be advanced as a possible explanation of the results.

TABLE 5

Calculated nominal values of ζ

Experiment No.	Cutting frequency ω_{21}^* (rad/sec)	Postcutting frequency ω_{11} (rad/sec)	Calculated ω_{21}	Calculated nominal ζ
1	772·8	791·7	813·2	0·31
2	769·7	—	—	—
3	772·8	798·0	819·3	0·33
4	763·4	779·1	800·9	0·30
5	1149·8	1200·1	1211·0	0·31
6	1161·8	1178·1	1192·3	0·22

Moreover, the above procedure may be advanced as a new way of estimating ζ. Many investigators have considered this important problem. Kalas [5] has measured the natural frequencies of the tool while cutting in order to obtain the dynamic characteristics of the process. Tlusty and Heczko [9] have improved Kalas's method by suggesting a design of a new flexible test rig (natural frequency of 200 Hz, almost the same as the one here). This rig allows measurements of damping coefficients directly from decay curves. The curves are obtained by hitting the tool while cutting, which is mounted on the flexible rig by an impact hammer, and comparing them with curves which were obtained without cutting.

Our experimental method, which is simpler, is basically equivalent to those mentioned above. However, in our experiments the flexible element in the system is the workpiece itself, and the value of ζ is determined from spectra, as opposed to using decay curves. It is suitable for turning of long slender workpieces.

5. SUMMARY AND CONCLUSIONS

In this paper a new dynamic cutting force model has been suggested for the turning of a long slender workpiece. The workpiece was assumed to be the flexible element, while the machine and the tool were considered rigid. The workpiece was described by a distributed parameter model, and the cutting force model included terms proportional to the workpiece displacement and velocity in the direction of the tool axis. The proposed model has then been studied both theoretically and experimentally.

In the cutting experiments only one typical natural frequency was consistently measured. This frequency was lower than the natural frequency of the workpiece without cutting. As a result of the experiments the main conclusions of the study are as follows.

(1) The model with damping was found to be in good agreement with the experimental results, for reasonable values of the process damping ratio ζ.

(2) The model prediction of two distinct natural frequencies (ω_{21}^* and ω_{11}) was not experimentally substantiated and further research is needed.

(3) The experimental procedure suggested here provides a new and convenient way of estimating the process damping ζ in turning of long slender workpieces.

REFERENCES

1. J. DATSKO 1966 *Material Properties and Manufacturing Processes.* Ann Arbor, MI: J. Datsko Consultants.
2. D. G. FLOM, R. KOMANDURI and M. LEE 1984 *Annual Review of Material Sciences* **19**, 231–278. High speed machining of metals.
3. J. P. GURNEY and S. A. TOBIAS 1961 *International Journal of MTDR* **1**, 148. A graphical method for the determination of the dynamic stability of machine tools.
4. N. H. HANNA and S. A. TOBIAS 1974 *ASME Journal of Engineering for Industry* 247–254. A theory of nonlinear regenerative chatter.
5. H. J. J. KALAS 1971 *CIRP Annals* **19**, 297–303. On the calculations of stability charts on the basis of the damping and stiffness of the cutting process.
6. R. KATZ, C. W. LEE, A. G. ULSOY and R. A. SCOTT 1987 *ASME Journal of Vibration, Acoustics, Stress and Reliability in Design* **109**, 361–365. Dynamic stability and response of a beam subject to a deflection dependent moving load.
7. R. KATZ, C. W. LEE, A. G. ULSOY and R. A. SCOTT 1988 *Journal of Sound and Vibration* **122**, 131–148. The dynamic response of a rotating shaft subject to a moving load.
8. H. E. MERRIT 1965 *ASME Journal of Engineering for Industry* 447–454. Theory of self-excited machine-tool chatter.
9. J. TLUSTY and O. HECZKO 1980 *SME 8th NAMRC Proceedings* **5**, 372–376. Improving tests of damping in the cutting process.

10. J. TLUSTY 1986 *ASME Journal of Engineering for Industry* **108**, 59-67. Dynamics of high speed machining.
11. S. A. TOBIAS 1965 *Machine Tool Vibration*. New York: John Wiley.
12. S. A. TOBIAS and W. FISHWICK 1958 *Transactions of ASME* **80**, 1079-1088. The chatter of lathe tools under orthogonal cutting conditions.

APPENDIX: NOMENCLATURE

A	cross sectional area of the workpiece
C_1, C_2	damping coefficients in the cutting force model
d	actual depth of cut
d_0	nominal depth of cut
EI	workpiece bending stiffness
f	feed rate
K_A, K_B	cutting force coefficients
K_1, K_2	elastic coefficients in the cutting force model
l	beam length
P	the cutting force
$\bar{P}$	the average component of the cutting force
U	workpiece lateral displacement relative to the lathe
v	axial velocity of the cutting force
z_i	discrete location along the workpiece
α, β	cutting force exponents
δP	incremental component of the cutting force
ζ	cutting process overall damping coefficient
ρ	mass density of the workpiece material
ω_1	natural frequency of a simply supported Euler–Bernoulli beam
ω_{11}	represents the natural frequency in the OX_2 direction (perpendicular to the tool)
ω_{21}	represents the natural frequency in the OX_1 (tool direction) when no damping is introduced
ω_{21}^*	represents the natural frequency in the OX_1 (tool direction) when process damping is introduced
$(\cdot)$	$d(\ )/dt$